2D-DOAE Using Temporal-Spatial Subspace Technique with Doppler Correction

Youssef Fayad, Member, IAENG, Caiyun Wang, and Qunsheng Cao

Abstract—In this paper a modified ESPRIT algorithm, which bases on time subspace (T-ESPRIT) and spatial subspace of estimate 2D-DOA (azimuth and elevation) of a radiated source, that can increase the estimation accuracy with low computational load is introduced. Using the algorithm, the planar array is divided into a multiple uniform sub-planar arrays with the common reference point, and the T-ESPRIT method is applied for each sub-array. Secondly, Doppler frequency shift (f_d) resulted from the target movement is estimated using displacement invariance technique (DIT). Then, in order to increase the estimation accuracy; the estimated Doppler frequency is used to correct the DOAE values according to target movement. Moreover, the proposed algorithm is combined the refined T-ESPRIT method with time differential of arrival (TDOA) technique to calculate an optimum DOA. It is found that the estimated results are better than the traditional ESPRIT methods leading to the estimator performance enhancement.

Index Terms— T-ESPRIT, Doppler frequency, TDOA, DOAE, Subspace.

I. Introduction

Estimating of direction-of-arrival (DOAE) is the creator of the tracking gate dimensions (the azimuth and the elevation) in the tracking while scan radars (TWS), a high DOAE errors means a high angle glint error which affects the accuracy of the tracking radar system. The DOAE of the multiple narrowband signals is an important process in array signal processing including sonar, radar, astronomy and mobile communications. The ESPRIT and its extracts have been widely studied in one-dimensional (1D) DOAE for uniform linear array (ULA), non-uniform linear array (NULA) [1]-[11], and also extended to two-dimensional (2D) DOAE [12]-[19]. All of these ESPRIT methods have been developed to upgrade the accuracy of DOAE with low calculation costs.

This paper presents a new modified algorithm based on time subspace (T-ESPRIT) [1], [2] and spatial subspace to reduce the computational costs of the 2D-DOAE (azimuth and elevation) of a radiated source which has been detected by a uniform planar array antenna with high accuracy. First, the spatial subspace is realized by arranging the main planar array as a multiple uniform sub-planar arrays related to the common reference point to get a unified phase shifts

Youssef Fayad. Author is with the College of Electronic and Information Engineering, Nanjing University of Aeronautics& Astronautics, Nanjing 210016, China (corresponding author to provide phone: 008618351005349; e-mail: youseffyad595@yahoo.com; youseffyad@nuaa.edu.cn).
Caiyun Wang. Author is with the College of Astronautics, Nanjing University of Aeronautics& Astronautics, Nanjing 210016, China (e-mail: wangcaiyun@nuaa.edu.cn).
Qunsheng Cao. Author is with the College of Electronic and Information Engineering, Nanjing University of Aeronautics& Astronautics, Nanjing 210016, China (e-mail:qunsheng @nuaa.edu.cn).

measurement point for all sub-arrays. The T-ESPRIT algorithm is applied on each sub-array separately, and in the same time with the others to realize time and space parallel processing, so that it reduces the non-linearity effect of model and decreases the computational time. Then, the target movement is detected via estimate its Doppler frequency by comparing the displacement invariances of transmitter and receiver arrays, which enables measurement of the sensor array displacement invariance fluctuation resulted from wavelength change induced by the target movement. It is worth mentioning that the subspace approach is also employed into DIT method to reduce the computations time. Moreover, the effect of Doppler frequency on the T-ESPRIT method is explained in order to refine the DOAE. Finally, the TDOA technique is applied and combined the multiple sub-arrays to calculate the optimum DOAE value at the reference antenna, which obtains to enhance the estimation accuracy and reduce computational load [20], [21].

The paper is organized as follows. In Section II, the Doppler correction for 2D T-ESPRIT technique and its combination with TDOA are introduced. In Section III, the simulation results are presented, and Section IV is conclusions.

II. Proposed Algorithm

A. The Measurement Model

In this model, the radiation propagates in straight lines due to isotropic and non-dispersive transmission medium assumption. Also, it is assumed that the sources as a far-field away the array. Consequently, the radiation impinging on the array is a summation of the plane waves. The signals are assumed to be narrow-band processes, and they can be considered to be sample functions of a stationary stochastic process or deterministic functions of time. Considering there are K narrow-band signals, and the center frequency f is assumed to have same $\omega_0 = 2\pi f$, for the kth signal can be written as

$$s_k(t) = E_k e^{j(\omega_0 t + \Psi_k)}, k = 1, 2, ..., \text{K} \qquad (1)$$

where $s_k(t)$ is the signal of the kth emitting source at time instant t, Ψ_k the carrier phase angles are assumed to be random variables, the each uniformly distributed on $[0,2\pi]$ and all statistically independent of each other.

Fig. 1 introduces a planar array oriented in *xoy* plane and arranged as sub-planar arrays and indexed with *N, G* along *y* and *x* directions respectively. Fig. 2 is shown a (*n, g*) sub-planar array where *n=1,...,N, g=1,...,G*, has elements indexed *L, I* along *y* and *x* directions respectively.

For any pairs (*i, l*), its coordinates with respect to the reference point (R.P) along *y* and *x* directions respectively are ($y^{il,n}$, $x^{il,g}$), where *i=1,...,I, l=1,...,L*.
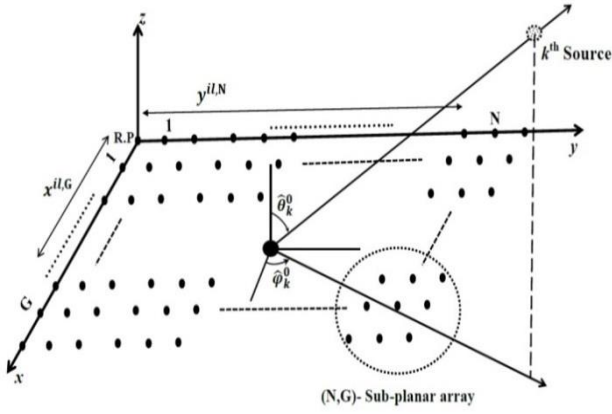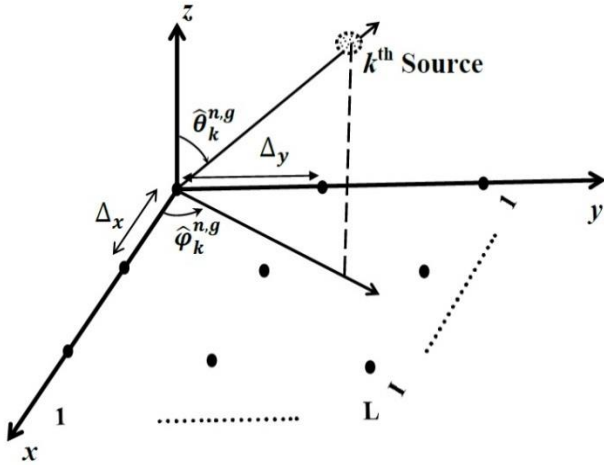
Fig. 1. Planar antenna array.

Fig. 2. Sub-Planar antenna array.

The space phase factors along x and y directions are expressed as

$$p_i\left(\theta_k^{n,g}, \varphi_k^{n,g}\right) \equiv p_i^k(n,g) = e^{j\frac{2\pi(i-1)\Delta_x}{\lambda} \sin\theta_k^{n,g} \cos\varphi_k^{n,g}} \quad (2)$$

$$x^{il,g} = \left((i-1)\cdot\Delta_x\right) + \left((g-1)\cdot I\cdot\Delta_x\right) \quad (3)$$

$$q_l\left(\theta_k^{n,g}, \varphi_k^{n,g}\right) \equiv q_l^k(n,g) = e^{j\frac{2\pi(l-1)\Delta_y}{\lambda} \sin\theta_k^{n,g} \sin\varphi_k^{n,g}} \quad (4)$$

$$y^{il,n} = \left((l-1)\cdot\Delta_y\right) + \left((n-1)\cdot L\cdot\Delta_y\right) \quad (5)$$

where $\left(\theta_k^{n,g}, \varphi_k^{n,g}\right)$ denote the kth source estimated elevation angle and azimuth angle respectively with respect to (n, g) sub-array, Δ_x and Δ_y are reference displacements between neighbor elements along x and y directions within any (n, g) sub-array also Δ_x and Δ_y are reference displacements between neighbor sub-arrays along x and y directions respectively, and λ is the wavelength of the signal. The receiving model can be expressed as:

$$[Z^{n,g}(t)] = [A^{n,g}][S(t)] + [W(t)] \quad (6)$$

where the matrices, $[S(t)], [A]$ and $[W(t)]$ are the receiving signal, transform factor for each sub-array, and AWGN (Additive White Gaussian Noise), respectively. They are given in subspace as follows

$$[Z^{n,g}(t)] = \left[z_{1,1}^{n,g}(t)\cdots z_{1,L}^{n,g}(t)\cdots z_{I,1}^{n,g}(t)\cdots z_{I,L}^{n,g}(t)\right]^T \quad (7)$$

$$[A^{n,g}] \stackrel{\text{def}}{=} \begin{bmatrix} u_k^T\left(\gamma_k, \eta_k, \theta_k^{n,g}, \varphi_k^{n,g}\right) \otimes p_i\left(\theta_k^{n,g}, \varphi_k^{n,g}\right) \\ \otimes q_l\left(\theta_k^{n,g}, \varphi_k^{n,g}\right) \end{bmatrix} \quad (8)$$

where $\otimes$ denotes the Kronker product. So, for any (n, g) sub-array

$$A\left(\theta_k^{n,g}, \varphi_k^{n,g}\right)$$
$$= [U_k^T p_1^k q_1^k \ U_k^T p_1^k q_2^k \ \dots \ U_k^T p_1^k q_L^k \ \ U_k^T p_2^k q_1^k \ \ U_k^T p_2^k q_2^k$$
$$\cdots U_k^T p_2^k q_L^k \ \cdots U_k^T p_I^k q_1^k \ U_k^T p_I^k q_2^k \cdots U_k^T p_I^k q_L^k]^T \quad (9)$$

where $p_i\left(\theta_k^{n,g}, \varphi_k^{n,g}\right)$, and $q_l\left(\theta_k^{n,g}, \varphi_k^{n,g}\right)$, are symbolized as p_i^k, q_l^k. And:

$$U_k^T = u_k\left(\gamma_k, \eta_k, \theta_k^{n,g}, \varphi_k^{n,g}\right)$$
$$= \begin{pmatrix} \sin\gamma_k \cos\theta_k^{n,g} \cos\varphi_k^{n,g} e^{j\eta_k} - \cos\gamma_k \sin\varphi_k^{n,g} \\ \sin\gamma_k \cos\theta_k^{n,g} \sin\varphi_k^{n,g} e^{j\eta_k} + \cos\gamma_k \cos\varphi_k^{n,g} \end{pmatrix}$$

$$(10)$$

$$[S(t)] \stackrel{\text{def}}{=} [s_1(t) \cdots \ \cdots s_K(t)]^T \quad (11)$$

$$[W(t)] = \left[w_{1,1}(t)\cdots w_{1,L}(t)\cdots w_{I,1}(t)\cdots w_{I,L}(t)\right]^T \quad (12)$$

The auxiliary polarization angle is defined as $\gamma \in [0, \pi/2]$, and the polarization phase difference is given as $\eta \in [-\pi, \pi]$. We omit (n, g) for simplicity. The whole data is divided into M snapshots at each time t_s second with sampling frequency f_s according to Nyquist law. Then it picks up enough data r enclosed by each snapshot m with time period $\tau = \frac{t_s}{r}$ as short as possible. So, from (6) each receiving signal measurement value through m^{th} subspace is given as

$$[z^m(\tau)] = [A]s^m(\tau) + [w^m(\tau)] \quad (13)$$

The index m runs as $m = 1, 2, \dots, M$ snapshots. Therefore, the whole space-time steering data matrix can be expressed as

$$Z \stackrel{\text{def}}{=}$$
$$\begin{bmatrix} z_{1,1}^1(0) & \dots & z_{1,1}^1(\tau_1)\dots\dots z_{1,1}^m(0) & \dots & z_{1,1}^m(\tau_1)\dots\dots z_{1,1}^M(0) & \dots & z_{1,1}^M(\tau_1) \\ \vdots & \ddots & \vdots & \ddots & \vdots & \ddots & \vdots \\ z_{I,L}^1(0) & \dots & z_{I,L}^1(\tau_1)\dots\dots z_{I,L}^m(0) & \dots & z_{I,L}^m(\tau_1)\dots\dots z_{I,L}^M(0) & \dots & z_{I,L}^M(\tau_1) \end{bmatrix}$$

$$(14)$$

Then

$$Z = [[z^1(\tau)] \ \dots \ [z^m(\tau)] \ \dots \ [z^M(\tau)]] \quad (15)$$

where $\tau_1 = \tau.(r-1)$, the dimension of $[Z]$ for the kth signal is $(2IL \times Mr)$. For the mth subspace data matrix can be expressed as

$$[z^m(\tau)] = \begin{bmatrix} z_{1,1}^m(0) & \dots & z_{1,1}^m(\tau_1) \\ \vdots & \ddots & \vdots \\ z_{I,L}^m(0) & \dots & z_{I,L}^m(\tau_1) \end{bmatrix} \quad (16)$$

For T-ESPRIT scheme the ESPRIT algorithm is used in an appropriate picked data represented in (14) for each (m) subspace given in (16). It is noted that (15) presents a parallel calculation for each subspace for the same sampling accuracy, however, the calculations load reduction and consequently saving time are achieved.

The ESPRIT algorithm is based on a covariance formulation that is

$$\hat{R}_{zz} \stackrel{\text{def}}{=} E[Z(\tau)Z^*(\tau)] = A\hat{R}_{ss}A^* + \sigma^2\Sigma_w \quad (17)$$

$$\hat{R}_{ss} = E[S(\tau)S^*(\tau)] \quad (18)$$

where $\hat{R}_{zz}$ is the correlation matrix of the sub-array output signal matrix, $\hat{R}_{ss}$ is the autocorrelation matrix of the signal. The subscript (*) denotes the complex conjugate transpose. The correlation matrix of $\hat{R}_{zz}$ can be done for eigenvalue decomposition as follow

$$\hat{R}_{zz} \stackrel{\text{def}}{=} \hat{E}_S \Lambda \hat{E}_S^* + \sigma^2 \hat{E}_N \Lambda \hat{E}_N^* \qquad (19)$$

where the eigenvalues are ordered $\lambda_1 > \lambda_2 > \cdots > \lambda_K > \lambda_{K+1} = \cdots = \lambda_{2(I \times L)} = \sigma^2$.

The eigenvectors $\hat{E}_S = [\hat{e}_1, \hat{e}_2, \cdots, \hat{e}_K]$ for larger K eigenvalues spans the signal subspace, the rest $2(I \times L) - K$ smaller eigenvalues $\hat{E}_N = [\hat{e}_{K+1}, \cdots, \hat{e}_{2(I \times L)}]$ spans the noise subspace which is orthogonal to the signal subspace. Therefore, there exists a unique nonsingular matrix Q, such that

$$\hat{E}_S = [A]Q = [u_k^T \otimes p_i(\theta_k, \varphi_k) \otimes q_l(\theta_k, \varphi_k)]Q \quad (20)$$

In (13) let A_{P1} and A_{P2} be the first and the last $2L \times (I-1)$ rows of A respectively, they differ by the factor $\Delta p_k = e^{j\frac{2\pi\Delta_x}{\lambda} \sin\theta_k \cos\varphi_k}$ along the x direction. So $A_{P2} = A_{P1}\emptyset_P$, where $\emptyset_P$ is the diagonal matrix with diagonal elements Δp_k. Consequently, $\hat{E}_{P1}$ and $\hat{E}_{P2}$ will be the first and the last $2L \times (I-1)$ sub-matrices formed from $\hat{E}_S$. Then the diagonal elements p_k of $\emptyset_P$ are the eigenvalues of the unique matrix $\Psi_P = Q^{-1}\emptyset_P Q$, that satisfies

$$\hat{E}_{P2} = \hat{E}_{P1}\Psi_P \qquad (21)$$

Similarly, the two $2I \times (L-1)$ sub-matrices A_{q1} and A_{q2} consist of the rows of A numbered $2L \times (i-1) + l$ and $2L \times (i-1) + l + 2$ respectively, differ by the space factors $\Delta q_k = e^{j\frac{2\pi\Delta_y}{\lambda}\sin\theta_k \sin\varphi_k}$ along the y direction, $l=1,...,2(L-1)$. Then $A_{q2} = A_{q1}\emptyset_q$ where $\emptyset_q$ is the diagonal matrix with diagonal elements Δq_k. Consequently, $\hat{E}_S$ forms the $2I \times (L-1)$ two sub-matrices $\hat{E}_{q1}$ and $\hat{E}_{q2}$. Then the diagonal elements Δq_k of $\emptyset_q$, are the eigenvalues of the unique matrix $\Psi_q = Q^{-1}\emptyset_q Q$, that satisfies

$$\hat{E}_{q2} = \hat{E}_{q1}\Psi_q \qquad (22)$$

Therefore, the arrival angles (θ_k, φ_k) for each sub-array can be calculated as

$$\theta_k = \sin^{-1}\left\{\frac{\lambda}{2\pi}\left[\left(\frac{arg(\Delta p_k)}{\Delta_x}\right)^2 + \left(\frac{arg(\Delta q_k)}{\Delta_y}\right)^2\right]^{1/2}\right\} \quad (23)$$

$$\varphi_k = \tan^{-1}\left[\frac{\Delta_x}{\Delta_y} \cdot \frac{arg(q_k)}{arg(p_k)}\right] \qquad (24)$$

B. Doppler Correction

The moving target echo signal is shifted by the Doppler frequency. The more accurate T-ESPRIT algorithm should consider the effect of the Doppler frequency shift due to the target movement. So,

$$arg(\Delta p_k) = \frac{2\pi}{\grave{\lambda}_x} \Delta_x \sin\theta_k \cos\varphi_k \qquad (25)$$

$$arg(\Delta q_k) = \frac{2\pi}{\grave{\lambda}_y} \Delta_y \sin\theta_k \sin\varphi_k \qquad (26)$$

where $\grave{\lambda}_x$ and $\grave{\lambda}_y$ are the wavelength components of the received wave into antenna plane and differ from the transmitted wavelength because of the Doppler frequency f_d caused by the target moving velocity $\vec{v}_s$ [22], [23], [24]. As shown in Fig. 3, it is obvious that the wavelength $\grave{\lambda}_x$ and $\grave{\lambda}_y$ have expressions caused by the velocity components v_x and v_y,

$$\grave{\lambda}_x = \frac{\lambda(c+v_x)}{c} \qquad (27)$$

$$\grave{\lambda}_y = \frac{\lambda(c+v_y)}{c} \qquad (28)$$

Substituting into (25), (26), then

$$arg(\Delta p_k) = \frac{2\pi c}{\lambda(c+v_x)} \Delta_x \sin\theta_k \cos\varphi_k \qquad (29)$$

$$arg(\Delta q_k) = \frac{2\pi c}{\lambda(c+v_y)} \Delta_y \sin\theta_k \sin\varphi_k \qquad (30)$$

where

$$v_x = |\vec{v}_s| \cos\alpha \sin\theta_k \cos\varphi_k \qquad (31)$$
$$v_y = |\vec{v}_s| \cos\alpha \sin\theta_k \sin\varphi_k \qquad (32)$$

And

$$|\vec{v}_s| = \frac{c \cdot f_d}{2f \cdot \cos\alpha} \qquad (33)$$

We define α as the angle between the direction of propagation and the target velocity vector $\vec{v}_s$, the value of α changes f_d sign indicating the target direction toward or away from the antenna position. From (29)-(32) the arrival angles (θ_k, φ_k) can be fine estimated from $(arg(p_k), arg(q_k))$ as follows

$$\theta_k = \sin^{-1}\left\{\left[\left(\frac{c \cdot arg(\Delta p_k)}{(2\pi c\Delta_x/\lambda) - arg(\Delta p_k) \cdot |\vec{v}_s| \cos\alpha}\right)^2 + \left(\frac{c \cdot arg(\Delta q_k)}{(2\pi c\Delta_y/\lambda) - (arg(\Delta q_k) \cdot |\vec{v}_s| \cos\alpha}\right)^2\right]^{1/2}\right\} \quad (34)$$

$$\varphi_k = \tan^{-1}\left[\frac{arg(\Delta q_k)}{arg(\Delta p_k)} \cdot \frac{(2\pi c\Delta_x/\lambda) - arg(\Delta p_k) \cdot |\vec{v}_s| \cos\alpha}{(2\pi c\Delta_y/\lambda) - arg(\Delta q_k) \cdot |\vec{v}_s| \cos\alpha}\right] \quad (35)$$
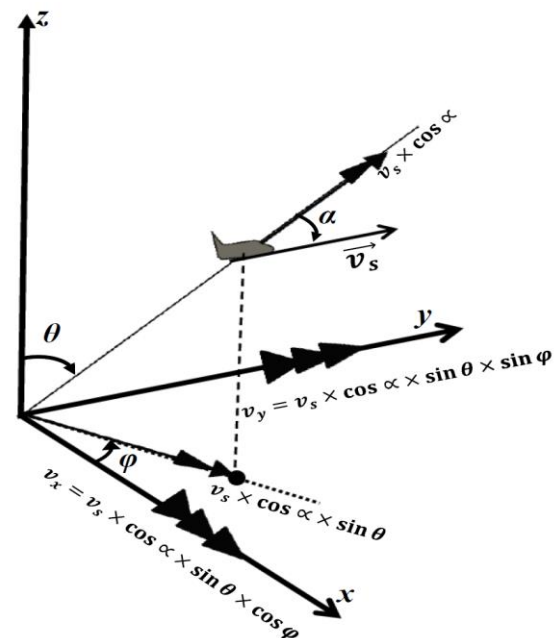

Fig. 3. Target linear velocity components into antenna plane

C. Doppler frequency estimation

In section *B* the effect of Doppler frequency on the moving target DOAE is modeled and incorporated into ESPRIT algorithm in order to increase the estimation accuracy. This Doppler frequency should be estimated with maintaining the low computational costs which is the important aim of this work. So, to realize this aim the T-ESPRIT technique which had been explained into (13)-(16), will be applied within Displacement Invariance Technique (DIT) to form T-DIT method. In T-DIT the wavelength change is measured via comparing the displacement invariance ratio $\left(\frac{\Delta_x}{\hat{\lambda}}, \frac{\Delta_y}{\hat{\lambda}}\right)$ of the received signal with the displacement invariance ratio $\left(\frac{\Delta_x}{\lambda}, \frac{\Delta_y}{\lambda}\right)$ of a signal generated from a transmitted signal sample and its phase. For the transmitted signal, where no Doppler effect, the departure space phase factors for each subspace are calculated as,

$$arg_d(\Delta p_k) = \frac{2\pi\Delta_x}{\lambda} sin\,\theta_k\,cos\,\varphi_k \qquad (36)$$

$$arg_d(\Delta q_k) = \frac{2\pi\Delta_y}{\lambda} sin\,\theta_k\,sin\,\varphi_k \qquad (37)$$

where departure and arrival angles are almost equal for the co-located planar array. From (29)-(35), the Doppler shift for each target (f_d^k) can be estimated as follows,

Substitute (33) into (31), (32) then into (29), (30),

$$arg_A(\Delta p_k) = \frac{2\pi\Delta_x}{\lambda} \cdot sin\,\theta_k\,cos\,\varphi_k \cdot \frac{2f}{2f+f_d^k\cdot sin\,\theta_k\,cos\,\varphi_k} \qquad (38)$$

$$arg_A(\Delta q_k) = \frac{2\pi\Delta_y}{\lambda} \cdot sin\,\theta_k\,sin\,\varphi_k \cdot \frac{2f}{2f+f_d^k\cdot sin\,\theta_k\,sin\,\varphi_k} \qquad (39)$$

Substitute (36)-(37) into (38), (39) respectively,

$$\frac{arg_d(\Delta p_k)}{arg_A(\Delta p_k)} = \frac{2f+f_d^k\cdot sin\,\theta_k\,cos\,\varphi_k}{2f} \qquad (40)$$

$$\frac{arg_d(\Delta q_k)}{arg_A(\Delta q_k)} = \frac{2f+f_d^k\cdot sin\,\theta_k\,sin\,\varphi_k}{2f} \qquad (41)$$

Thus,

$$f_d^k = \left(\frac{2\cdot f}{sin\,\theta_k}\right) \cdot \left[\left(\frac{arg_d(\Delta p_k)}{arg_A(\Delta p_k)}-1\right)^2 + \left(\frac{arg_d(\Delta q_k)}{arg_A(\Delta q_k)}-1\right)^2\right]^{1/2} \qquad (42)$$

The variable θ_k is the coarse estimated value of the elevation angle stated from (23). From Figure.3 it is clear that the target direction estimation depends on v_y moving direction and θ_k, their values are listed in Table I.

TABLE I
TARGET DIRECTIONAL JUDGMENT

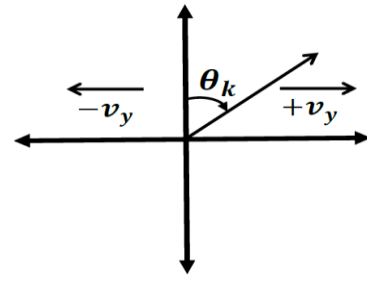| $sin(\theta_k)$	v_y	$v_y \cdot sin(\theta_k)$	Target direction
+ ve	+ ve	+ ve	Away from antenna
+ ve	- ve	- ve	Close to antenna
- ve	+ ve	- ve	Close to antenna
- ve	- ve	+ ve	Away from antenna

Fig. 4. Target direction dependence on v_y, and θ_k.

It is clear from Figure.4 that our main purpose is to determine v_y sign (the target direction). Substituted (37) into (30), then it has follow,

$$v_y = c \cdot \left(\frac{arg_d(\Delta q_k)}{arg_A(\Delta q_k)} - 1\right) \qquad (43)$$

So,

$$\begin{cases} arg_A(\Delta q_k) < arg_d(\Delta q_k), & if\ v_y = +ve \\ arg_A(\Delta q_k) > arg_d(\Delta q_k), & if\ v_y = -ve \\ arg_A(\Delta q_k) = arg_d(\Delta q_k), & if\ v_y = 0 \end{cases} \qquad (44)$$

and $\hat{\lambda}_x = \hat{\lambda}_y = \lambda$ for stationary target.
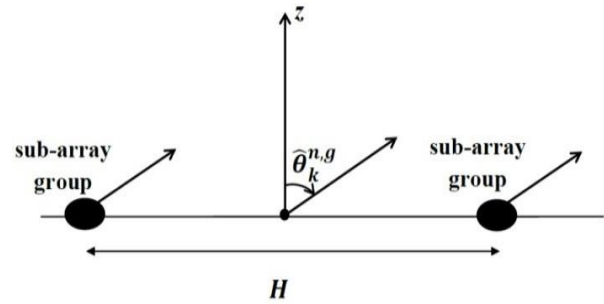
D. Optimal DOAE Calculation

Fig. 5. Arrangement of sub-Planar pair.

For sub-Planar pair shown in Fig. 5, the TDOA (δ^{ng}) for the kth received signal is calculated as follow [25]

$$\delta_k^{ng} = \frac{H}{c} sin\,\hat{\theta}_k^{ng} \qquad (45)$$

where c is the wave velocity (3×10^8 m/sec) and H is the distance between any (n, g) sub-array groups as shown in Fig. 5. For the sub-planar groups shown in Fig. 6, the TDOA between group (1, 1) and group (N, G) for the kth source is denoted by δ_k^{1G}, and the TDOA between group (N, 1) and group (1, G) for the kth source is denoted by δ_k^{N1}.

So, from (45)

$$\delta_k^{1G} = \frac{H}{c} sin\,\hat{\theta}_k^{1G} \qquad (46)$$

$$\delta_k^{N1} = \frac{H}{c} sin\,\hat{\theta}_k^{N1} \qquad (47)$$

And

$$H = \sqrt{(H_x)^2 + \left(H_y\right)^2} \qquad (48)$$

where H_x, H_y are the distance between the first and last sub-array arranged along *x* and *y* directions respectively.
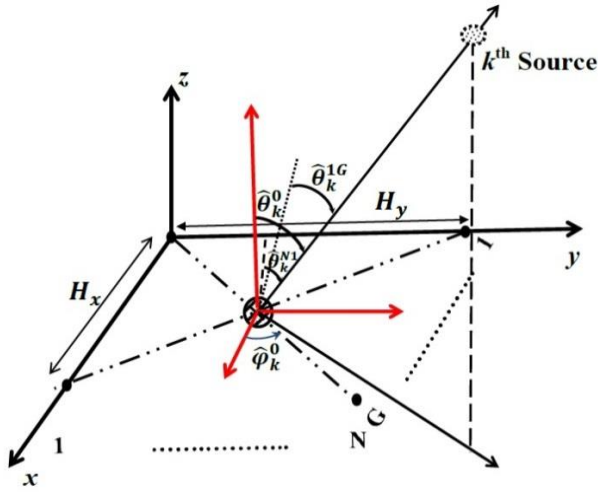
Fig. 6.   Arrangement of sub-planar groups.

And

$$H_x = x_c^{g=G} - x_c^{g=1} \qquad (49)$$

$$H_y = y_c^{n=N} - y_c^{n=1} \qquad (50)$$

From (3), and (5)

$$x_c^g = \left(\frac{(I-1)}{2} \cdot \Delta_x\right) + \left((g-1) \cdot I \cdot \Delta_x\right) \qquad (51)$$

$$y_c^n = \left(\frac{(L-1)}{2} \cdot \Delta_y\right) + \left((n-1) \cdot L \cdot \Delta_y\right) \qquad (52)$$

And

$$\hat{\theta}_k^{1G} = \frac{\hat{\theta}_k^{1,1} + \hat{\theta}_k^{N,G}}{2} \qquad (53)$$

$$\hat{\theta}_k^{N1} = \frac{\hat{\theta}_k^{N,1} + \hat{\theta}_k^{1,G}}{2} \qquad (54)$$

Where the value of θ_k for any (n, g) sub-array group was estimated as in (34). Substitute (48-54) into (46), (47) the kth received signal TDOA $(\delta_k^{1G}, \delta_k^{N1})$ are obtained. So, as shown in Fig.6 the optimal DOAE values $(\theta_k^0, \varphi_k^0)$ are measured at the center of the sub-array groups which is located in the cross point of the straight lines pass through group $(1, 1)$ and group (N, G) and through group $(N, 1)$ and group $(1, G)$. Thus, $(\theta_k^0, \varphi_k^0)$ values can be represented in terms of $(\hat{\theta}_k^{1G}, \hat{\theta}_k^{N1})$ as follow [25], [26]

$$\sin \hat{\theta}_k^{1G} = \sin \hat{\theta}_k^0 \sin \hat{\varphi}_k^0 = \frac{c\delta_k^{1G}}{H} \qquad (55)$$

$$\sin \hat{\theta}_k^{N1} = \sin \hat{\theta}_k^0 \cos \hat{\varphi}_k^0 = \frac{c\delta_k^{N1}}{H} \qquad (56)$$

From (55), (56) the optimal DOAE values are

$$\hat{\varphi}_k^0 = \tan^{-1}\left(\frac{\delta_k^{1G}}{\delta_k^{N1}}\right) \qquad (57)$$

$$\hat{\theta}_k^0 = \sin^{-1}\left(\frac{c}{H}\sqrt{(\delta_k^{1G})^2 + (\delta_k^{N1})^2}\right) \qquad (58)$$

III.   SIMULATION RESULTS

Considering the 2D-DOAE process with the AWGN, the parameters are given $f_s = 25$ MHz. Assuming total 25 temporal snapshots, pickup enclosed data $r =20$ times, and

200 independent Monte Carlo simulations. In order to validate the proposed method, it has been used in the planar case with number of elements, such as $(I, L) = (3, 3)$, $(N, G) = (2, 2)$ with displacement values $\Delta_x = \Delta_y = \lambda/2$, with initial values of $\theta=45^o$ and $\varphi=60^o$. It is found that the computational load has been decreased as a result of reducing the measurement matrix dimension to $[2IL \times r]$ instead of $[2(IG)(LN) \times Mr]$. Table. II represents the computational time and complexity of the proposed method in term of number of flip-flops. It is obvious that the computational load has been reduced as a result of employing time subspace and spatial subspace to enable a simultaneous processing for M subspaces with each has r snapshots for sub-array with (I, L) elements instead of processing for one space has a large number of snapshots d, $(d=Mr)$ snapshots for array with (IG, LN) elements.

TABLE II
COMPUTATION TIME AND COMPLEXITY COMPARISON

Algorithm Computational	Conventional ESPRIT	Proposed algorithm
time (msec)	17.7	1.14
complexity	$O([4d(IGLN)^2 + 8(IGLN)^3])$	$O([M+4r(IL)^2 + 8(IL)^3])$

Fig. 7 is plotted the RMSEs of the proposed algorithm (T-ESPRIT with spatial subspace) by dividing the planar array into two sub-planar arrays with $(I, L) = (3, 3)$, $(N, G) = (2, 2)$. Results shown in Fig. 7 indicate that the proposed algorithm errors are getting closer to the CRB as a result of applying subspace concept with Doppler correction.
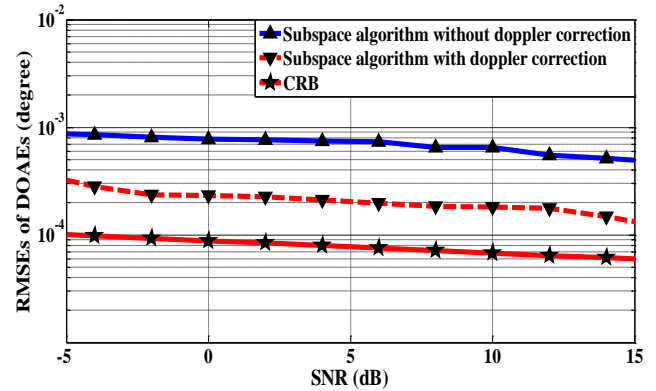

Fig. 7.   RMSEs vs. SNR for the proposed (T-ESPRIT & spatial subspace) combined algorithm.

Additionally, in order to introduce the improvement in the computation time compared to estimate Doppler frequency via using the FFT method, Table. III represents a comparison between the proposed method computation time and the different FFT methods mentioned in [27].

TABLE III
COMPARISON OF THE REQUIRED COMPUTATION TIME

Algorithms	Computation time (Sec)
Direct calculation	80.3702
FFT method	1.5112
ZFFT method	0.1604
PWZFFT method	0.0835
Proposed T-DIT method	0.00926

Results in Table III show that the computation time is reduced to 11.09% compared to the best computation time which has been realized via using PWZFFT method [27]. This improvement has been realized because of using the temporal subspaces concept which enables parallel processing. The accuracy improvement of the 2D-DOAE using proposed algorithm has been verified by comparing the resulted RMSEs with the RMSEs of 2D-Beamspace ESPRIT and the ESPRIT-Like algorithms used in [15], [17] respectively.
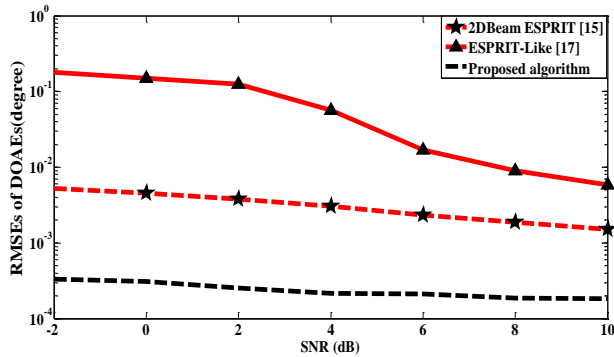

Fig. 8. RMSEs vs. SNR for the proposed algorithm and Beam space-ESPRIT methods.

A comparison results displayed in Fig. 8 show that the proposed algorithm has a better performance, especially at a low SNR. This upgrade has been realized due to the increase of DOAE accuracy when combining the T-ESPRIT with spatial subspace algorithm applying the subspace approach which decreases the errors caused by the model non-linearity effect and increases the resolution of phase deference measurement. Additionally, this improvement is due to Doppler correction which reduces the DOAE uncertainty associated with effect of the target movement.

From Table. II, it has been found that the proposed algorithm requires $O([M+4r(IL)^2+8(IL)^3])$ flops [28], while the conventional ESPRIT algorithm needs $O([4d(IGLN)^2+8(IGLN)^3])$ flops. The proposed ESPRIT algorithm requires about 6% of the computational time compared with that of the classical ESPRIT algorithm.

Clearly we can figure out that the process of combining between the refined T-ESPRIT algorithm and the spatial subspace algorithm achieved success into increasing the DOAE accuracy with low computational load. Simply, the developed ESPRIT method improves the estimator performance.

IV. CONCLUSIONS

In this paper, a new ESPRIT method is developed based on the concept of subspace. Firstly, T-ESPRIT method algorithm is used to estimate DOA for each sub-array realizing time subspace concept. Secondly, T-ESPRIT DOA estimated value is corrected according to Doppler frequency resulted from target movement which is estimated using T-DIT method. Finally, the modified T-ESPRIT method is combined with TDOA algorithm to compute the optimal DOAE value which was estimated with different sub-arrays to realize spatial subspace concept. It has been found that the estimation accuracy has been increased with low computational load; also the computational time has been

reduced about 88% for Doppler estimation and 94% for DOAE, which consequently enhance the estimator performance.

REFERENCES

[1] Youssef Fayad, Caiyun Wang, Qunsheng Cao Alaa El-Din Sayed Hafez, "A developed ESPRIT algorithm for DOA estimation," *Frequenz*, vol.69, no. 3, pp. 263 – 269, 2015.

[2] Youssef Fayad, Caiyun Wang, Alaa El-Din Sayed Hafez, Qunsheng Cao, "Direction of Arrival Estimation Using Novel ESPRIT Method for Localization and Tracking Radar Systems," Proceedings of the *IEEE 11th International Bhurban Conference on Applied Sciences & Technology (IBCAST)*, Islamabad, Pakistan, January 14–18, 2014, pp. 396-398.

[3] Nordkvist N. and Sanyal A.K.,"Attitude Feedback Tracking with Optimal Attitude State Estimation," *American Control Conference*, 2010, pp.2861-2866.

[4] Richard Roy, A. Paulraj and Thomas Kailath, "ESPRIT-Estimation of Signal Parameters via Rotational Invariance Techniques, acoustic, Speech, and signal processing," *IEEE international conference on ICASSP*, 1986, vol. 11. pp. 2495-2498.

[5] R. H. Roy, "ESPRIT-Estimation of signal parameters via rotational invariance techniques," Ph.D. dissertation, Stanford Univ., Stanford, CA, 1987.

[6] Richard Roy and Thomas Kailath, "ESPRIT-Estimation of Signal Parameters Via Rotational Invariance Techniques," *IEEE Transaction on acoustic*, *Speech, and signal processing*, vol. 37, no. 7, pp. 984-995, 1989.

[7] Z. I. Khan, R.A. Awang, A. A. Sulaiman, M. H. Jusoh, N. H. Baba, M. MD. Kamal and N. I. Khan, "Performance Analysis for Estimation of Signal Parameters via Rotational Invariance Technique (ESPRIT) in estimating Direction of Arrival for linear array antenna," *IEEE international RF And Microwave conference*, Kuala Lumpur, Malaysia, December 2-4, 2008, pp.530-533.

[8] Aweke N. Lemma, Alle-Jan van der Veen and Ed F. Deprettere, "Joint Angle-Frequency Estimation using Multi-Resolution ESPRIT," *Proceedings of the IEEE International Conference on Acoustics, Speech and Signal Processing*, 1998, vol.4, pp. 1957-1960.

[9] Gui-min Xu, Jian-guo Huang "Multi-resolution Parameters Estimation for Polarization Sensitivity Array," *IEEE International Symposium on Knowledge Acquisition and Modeling Workshop, KAM*, 2008, pp. 180-183.

[10] Volodymyr Vasylyshyn, "Direction of Arrival Estimation using ESPRIT with Sparse Arrays," *EUMA-6th European Radar Conference*, 30 September – 2 October, Rome, Italy, 2009, pp.246-249.

[11] Aweke N. Lemma, Alle-Jan van der Veen and Ed F. Deprettere, "Multiresolution ESPRIT Algorithm," *IEEE Transaction on signal processing*, vol. 47, no. 6, pp. 1722-1726, 1999.

[12] F. Gao, A. B. Gershman, "A generalized ESPRIT approach to direction of arrival estimation," *IEEE Signal Processing Letters*, vol. 12, no. 3, pp. 254 – 257, 2005.

[13] Youssef Fayad, Caiyun Wang, and Qunsheng Cao, "Doppler Correction for Spatial Subspace Technique," *Lecture Notes in Engineering and Computer Science: Proceedings of The World Congress on Engineering and Computer Science 2015, WCECS 2015, 21-23 October 2015, San Francisco, USA*, pp. 508-513.

[14] Youssef Fayad, Caiyun Wang, and Qunsheng Cao, "A Developed ESPRIT for Moving Target 2D-DOAE," *Engineering Letters, to be published.*

[15] Cherian P. Mathews, Martin Haardt, Michal D. Zoltowski, "performance analysis of closed-form, ESPRIT based 2-D angle estimator for rectangular arrays," *IEEE Signal Processing Letters*, vol. 3, no. 4, pp. 124 – 126, 1996.

[16] Y. Zhang, Z. Ye, X. Xu, and J. Cui, "Estimation of two-dimensional direction-of-arrival for uncorrelated and coherent signals with low complexity," *IET Radar Sonar Navigation*, vol. 4, no.4, pp.507-519, 2010.

[17] Fang-Jiong Chen, Sam Kwong, Chi - Wah Kok, "ESPRIT-Like Two-Dimensional DOA Estimation for Coherent Signals," *IEEE Transactions on Aerospace and Electronic Systems* vol. 46 , no. 3 , pp. 1477 – 1484, 2010.

[18] Jiang Hui, Yang Gang "an improved algorithm of ESPRIT for signal DOA estimation," *International conference on industrial control and electronics engineering*, Aug 23-25, 2012, pp.317 – 320.

[19] X. Xu, Z. Ye, "Two-dimensional direction of arrival estimation by exploiting the symmetric configuration of uniform rectangular array," *IET Radar Sonar Navigation*, vol. 6, no.5, pp.307-313, 2012.

[20] Fawaz Alassery, Walid K. M. Ahmed, Mohsen Sarraf, and Victor Lawrence, "A Low Computational Complexity Statistical Discrimination Algorithm for Collision Detection in Wireless Sensor Networks," *IAENG International Journal of Computer Science*, vol. 41, no.3, pp.204-211, 2014.

[21] Weiya Yue, John Franco, "A New Way to Reduce Computing in Navigation Algorithm", *Engineering Letters*, vol.18, no.4, pp.341-350, 2010.

[22] F. B. BERGER, "The Nature of Doppler Velocity Measurement," *IRE transactions on aeronautical and navigational electronics*, vol. ANE-4, no. 3, pp. 103 – 112, 1957.

[23] A. Nabavizadeh, M. W. Urban, R. R. Kinnick, and M. Fatemi, "Velocity Measurement by Vibro-Acoustic Doppler," *IEEE Transactions on Ultrasonics, Ferroelectrics, and Frequency Control*, vol. 59, no. 4, pp. 752 - 765 , 2012.

[24] A-level Physics (Advancing Physics), http://en.wikibooks.org. , 2015.

[25] Ye Tian, Akiyoshi Tatematsu, Kazuo Tanabe, and Kiyotomi Miyajima, "Development of Locating System of Pulsed Electromagnetic Interference Source Based on Advanced TDOA Estimation Method," *IEEE Trans. electromagnetic compatibility*, vol. 56, no. 6, pp.1326-1334, 2014.

[26] T. Tantisattayakul, K. Masugata, I. Kitamura, K. Kontani, "Broadband VHF sources locating system using arrival-time differences for mapping of lightning discharge process," *Journal of Atmospheric Solar-Terrestrial Phys.*, vol. 67, pp. 1031–1039, 2005.

[27] R. Tao, W. -Q. Zhang, and E. -Q. Chen "Two-stage method for joint time delay and Doppler shift estimation," IET Radar Sonar Navigation, vol. 2, no.1, pp.71-77, 2008.

[28] Cheng Qian, Lei Huang and H.C. So "Computationally efficient ESPRIT algorithm for direction-of-arrival estimation based on Nyström method," *Signal Processing*, vol. 94, pp.74-80, 2014.

Youssef Fayad (Alexandria Egypt, 4/9/1975) received the B.S. In electronic engineering and the M.S. in communications and electronics from faculty of engineering, Alexandria University, Egypt, in 1997, 2010 respectively. He is currently in Ph.D. degree in radar system in Nanjing University of Aeronautics and Astronautics, college of electronic and information engineering, Nanjing, china. He is an IAENG Member, and a Student Member of IEEE, he is also worked as an Assistant Lecturer in Air Defense College, Egypt. Mr. Fayad research interests in antenna and radar signal processing.

Caiyun Wang was born in Shanxi, China, on September 30, 1975. She graduated in 1996 with a B.S. degree and in 1999 with a M.S. degree. She received the Ph.D. degree in signal and information processing from Beihang University, Beijing, China, in 2008. She is currently an associate professor with the College of Astronautics , Nanjing University of Aeronautics and Astronautics (NUAA). Her major research interests are in the fields of radar automatic target recognition (RATA), radar signal processing, and adaptive signal processing, and pattern recognition.

Qunsheng Cao received his Ph.D. in electrical engineering from The Hong Kong Polytechnic University in 2001. From 2001 to 2005 he worked as a Research Associate in the Department of Electrical Engineering, University of Illinois at Urbana-Champaign and at the Army High Performance Computing Research Center (AHPCRC), University of Minnesota. In2006, Dr. Cao joined the Nanjing University of Aeronautics and Astronautics (NUAA), China, as a Professor of electrical engineering. Dr.Cao's current research interests are in computational electromagnetics, antenna and microwave technology and the radar signal processing. Dr. Cao has published more than 120 academic papers in refereed journals and conference proceedings.